JOURNAL OF BACTERIOLOGY, Aug. 1996, p. 4522–4529 Vol. 178, No. 15
0021-9193/96/$04.00+0

The *Alcaligenes eutrophus* Membrane-Bound Hydrogenase Gene Locus Encodes Functions Involved in Maturation and Electron Transport Coupling

MICHAEL BERNHARD,[1] EDWARD SCHWARTZ,[1] JENS RIETDORF,[2] AND BÄRBEL FRIEDRICH[1]*

Institut für Biologie der Humboldt-Universität zu Berlin[1] and Institut für Pflanzenphysiologie und Mikrobiologie der Freien Universität Berlin,[2] Berlin, Germany

Received 5 February 1996/Accepted 27 May 1996

Alcaligenes eutrophus **H16 produces two [NiFe] hydrogenases which catalyze the oxidation of hydrogen and enable the organism to utilize H_2 as the sole energy source. The genes (*hoxK* and *hoxG*) for the heterodimeric, membrane-bound hydrogenase (MBH) are located adjacent to a series of eight accessory genes (*hoxZ*, *hoxM*, *hoxL*, *hoxO*, *hoxQ*, *hoxR*, *hoxT*, and *hoxV*). In the present study, we generated a set of isogenic mutants with in-frame deletions in the two structural genes and in each of the eight accessory genes. The resulting mutants can be grouped into two classes on the basis of the H_2-oxidizing activity of the MBH. Class I mutants (*hoxK*Δ, *hoxG*Δ, *hoxM*Δ, *hoxO*Δ, and *hoxQ*Δ) were totally devoid of MBH-mediated, H_2-oxidizing activity. The *hoxM* deletion strain was the only mutant in our collection which was completely blocked in carboxy-terminal processing of large subunit HoxG, indicating that *hoxM* encodes a specific protease. Class II mutants (*hoxZ*Δ, *hoxL*Δ, *hoxR*Δ, *hoxT*Δ, and *hoxV*Δ) contained residual amounts of MBH activity in the membrane fraction of the extracts. Immunochemical analysis and ^{63}Ni incorporation experiments revealed that the mutations affect various steps in MBH maturation. A lesion in *hoxZ* led to the production of a soluble MBH which was highly active with redox dye.**

The gram-negative bacterium *Alcaligenes eutrophus* H16 is able to grow heterotrophically on various organic substrates or autotrophically with hydrogen as the energy source. The oxidation of molecular hydrogen is catalyzed by two metalloenzymes: a cytoplasmic, heterotetrameric NAD-reducing hydrogenase (SH) (38) and a membrane-bound heterodimeric hydrogenase (MBH) (36) which is linked to the electron transport chain. Both enzymes belong to the family of [NiFe] hydrogenases (reviewed in reference 12).

The genes for the two enzymes form separate operons located about 50 kb apart on megaplasmid pHG1. The four subunits of the SH are coded for by genes *hoxF*, *hoxU*, *hoxY*, and *hoxH* (43). *hoxK* and *hoxG* encode the small (HoxK) and large (HoxG) subunits of the MBH, respectively (20). Sequencing of the MBH locus revealed a series of eight major open reading frames (ORFs) 3′ of the structural genes. The deduced products of these ORFs were found to be homologous to proteins coded for by genes adjacent to hydrogenase determinants in other H_2-oxidizing bacteria (12, 46). This result pointed to a conserved hydrogenase-related function for the eight ORFs. Complementation studies showed that plasmids carrying MBH structural genes *hoxK* and *hoxG* but lacking the downstream ORFs failed to complement a mutant with a large deletion in the MBH locus. In contrast, plasmids harboring the structural genes and an intact set of accessory genes restored near-wild-type activity. This result indicated that at least some of the ORFs encode biological functions required for MBH synthesis. We therefore gave the ORFs the designations *hoxZ*, *hoxM*, *hoxL*, *hoxO*, *hoxQ*, *hoxR*, *hoxT*, and *hoxV* (20).

Immunological analysis showed that *A. eutrophus* strains which lacked a complete set of accessory genes and hence were devoid of MBH activity nevertheless produced normal levels of MBH polypeptides. Furthermore, a strain with a defect in the downstream *hoxM* gene contained MBH protein, but the enzyme was not attached to the cytoplasmic membrane, as in wild-type cells. Parallel studies carried out in our laboratory led to the discovery that both the HoxK subunit and the HoxG subunit undergo modifications which manifest themselves as alterations in electrophoretic mobility. In the case of HoxK, proteolytic removal of an N-terminal signal peptide is the basis of the change in mobility (19). We suspect that HoxG undergoes C-terminal proteolytic processing analogous to that demonstrated for the HoxH subunit of the SH (41). Recently, we reported a genetic analysis of the *A. eutrophus hyp* genes. Three of the six *hyp* genes were shown to be essential for the incorporation of nickel into HoxG. The block in nickel incorporation in the *hyp* mutants curtails modification of HoxG. Thus, curtailment of nickel incorporation seems to arrest maturation at an early stage (7).

Taken together, the findings summarized above indicate that MBH maturation is a complex process involving several specialized gene products. In this communication, we present the results of a systematic investigation of the accessory genes of the MBH region. To facilitate the unambiguous assignment of phenotypes, we introduced defined in-frame deletions into each of the genes via an allelic exchange strategy refined in our laboratory (24). We determined the effect of these mutations on MBH activity.

MATERIALS AND METHODS

Strains and plasmids. The bacterial strains and plasmids used in this study are listed in Table 1. *Escherichia coli* XL1-Blue (Stratagene Cloning System, Inc.) was used as a host in standard cloning procedures, and *E. coli* JM109 (48) was used for constructs involving plasmid pMAL-c2. *E. coli* S17-1 (39) served as a donor in conjugative transfers. *A. eutrophus* H16 is the wild-type strain harboring megaplasmid pHG1. Strains carrying the letters HF are derivatives of *A. eutrophus* H16.

* Corresponding author. Mailing address: Institut für Biologie, Humboldt-Universität zu Berlin, Chausseestr. 117, D-10115 Berlin, Germany. Electronic mail address: Baerbel-Friedrich@rz.hu-berlin.de.

TABLE 1. Bacterial strains and plasmids used in this study

Strain or plasmid	Genotype and/or characteristics	Source or reference
Alcaligenes eutrophus		
H16	Wild type	DSM428, ATCC 17699
HF345	*hoxM*ΔR4	This work
HF359	*hoxG*ΔR4	This work
HF361	*hoxR*ΔR14	This work
HF363	*hoxT*ΔR1	This work
HF365	*hoxV*ΔR1	This work
HF388	*hoxH*Δ	7
HF403	*hoxK*ΔR9	This work
HF404	*hoxK*ΔleaderR30	This work
HF405	*hoxZ*ΔR13	This work
HF406	*hoxL*ΔR3	This work
HF407	*hoxO*ΔR8	This work
HF408	*hoxQ*ΔR2	This work
Escherichia coli		
S17-1	Tra^+; *recA pro thi hsdR chr*::RP4-2	39
XL1-Blue	*recA1 endA1 gyrA96 thi-1 hsdR17 supE44 relA1 lac* [F′ *proAB lacI*^{q} *lacZ*ΔM15 Tn*10*(Tc^r)]	Stratagene Cloning Systems
JM109	F′ *traD36 lacI*^{q} *lacZ*ΔM15 *proAB recA1 thi gyrA96 endA1 hsdR17 relA1 supE44*	48
Plasmids		
pBluescript I SK+	Ap^r *lacZ′*, T7 ϕ10 promoter, f1 *ori*	Stratagene Cloning Systems
pACYC177	Ap^r, Km^r, ColE1 *ori*	3
pMAL-c2	Ap^r, ColE1 *ori*	New England Biolabs
pJD1	Km^r, $oriT_{RP4}$, ColE1 *ori*	7
pLO1	Km^r, *sacB*, $oriT_{RP4}$, ColE1 *ori*	24
pLO2	Km^r, *sacB*, $oriT_{RP4}$, ColE1 *ori*	24
pCH182	4.8-kb *Pst*I-*Sal*I fragment of pGE53 in pTZ19R	C. Kortlüke and B. Friedrich
pCH305	1.6-kb *Eco*RI-*Pst*I fragment of pGE44 in pBluescriptSK+	M. Eitinger and B. Friedrich
pCH311	1.1-kb *Pst*I-*Sma*I fragment of pGE195 in pBluescriptSK+	20
pCH409	2.6-kb *Mam*I-*Pst*I fragment of pCH327 in pJD1	This work
pCH410	1.2-kb *Sca*I-*Eco*RI fragment of pCH409 reinserted between the *Sal*I (end-polished) and *Eco*RI sites of the same plasmid (180-bp deletion in *hoxM*)	This work
pCH411	2-kb *Sph*I fragment of pCH410 in pLO1 (*hoxM*Δ)	This work
pCH423	1.6-kb *Nde*I-*Bsa*BI fragment of pCH182 in pTZ19R (1,524-bp deletion in *hoxG*)	This work
pCH424	2.2-kb *Sal*I-*Sma*I fragment of pCH423 in pLO1 (*hoxG*Δ)	This work
pCH425	1.5-kb *Sal*I-*Nhe*I fragment of pGE195 in pLO2	This work
pCH426	Derivative of pCH425 from which a 195-bp *Bst*BI-*Rsr*II fragment has been deleted (*hoxR*Δ)	This work
pCH427	1.7-kb *Asp*I-*Sph*I (Klenow-treated) fragment in pLO1	This work
pCH428	Derivative of pCH427 from which a 165-bp *Sal*I-*Eco*RV (Klenow-treated) fragment has been deleted (*hoxT*Δ)	This work
pCH429	Derivative of pCH305 from which a 429-bp *Nco*I-*Bsp*EI fragment has been deleted (*hoxV*Δ)	This work
pCH430	1.1-kb *Xba*I-*Eco*RV fragment in pLO1 (*hoxV*Δ)	This work
pCH460	3.5-kb *Eco*RI (Klenow-treated) fragment of pGE195 in pACYC177	This work
pCH461	Derivative of pCH460 carrying a PCR-generated, 274-bp *Fsp*I fragment in place of the corresponding wild-type fragment (621-bp deletion in *hoxZ*)	This work
pCH462	2.7-kb *Eco*RV fragment of pGE195 in pMAL	This work
pCH463	Derivative of pCH462 carrying a PCR-generated, 520-bp *Xho*I-*Sph*I fragment in place of a 616-bp *Xho*I-*Sph*I fragment (96-bp deletion in *hoxL*)	This work
pCH464	0.9-kb *Sca*I-*Sph*I fragment in pLO1 (*hoxL*Δ)	This work
pCH465	1.2-kb *Sca*I-*Sal*I fragment in pLO1 (*hoxZ*Δ)	This work
pCH466	2.7-kb *Eco*RV fragment of pGE195 in pBluescriptSK+	This work
pCH467	Derivative of pCH466 from which a 306-bp *Nae*I fragment has been deleted (deletion in *hoxO*)	This work
pCH468	2.4-kb *Sca*I-*Xba*I fragment in pLO1 (*hoxO*Δ)	This work
pCH469	2.5-kb *Sca*I-*Nhe*I fragment of pGE195 in pACYC177	This work
pCH470	Derivative of pCH469 carrying 34-bp synthetic linker in place of a 775-bp *Eco*RI-*Sfi*I fragment (741-bp deletion in *hoxQ*)	This work
pCH471	1.9-kb *Hin*dIII (Klenow-treated)-*Nhe*I fragment in pLO1 (*hoxQ*Δ)	This work
pCH497	2-kb *Bam*HI (Klenow-treated) fragment in pBluescriptSK+	This work
pCH498	Derivative of pCH497 from which a 438-bp *Nae*I fragment has been deleted (*hoxK*Δ)	This work
pCH499	2-kb *Pvu*II-*Ssp*I fragment in pLO2 (*hoxK*Δ)	This work
pCH500	Derivative of pCH497 carrying a 490-bp *Fsp*I-*Nae*I fragment of pCH311 in place of a 526-bp *Eco*RV-*Sca*I fragment (36-bp deletion in the *hoxK* leader sequence)	This work
pCH501	2.3-kb *Ssp*I fragment of pCH500 in pLO2 (*hoxK*Δleader)	This work
pGE151	Derivative of pRK404	20
pGE195	9.2-kb *Pst*I fragment of pHG1 in pVK101	20

Defined in-frame deletion alleles for use in allelic exchange mutagenesis were constructed in subcloned wild-type *hox* sequences. The deletions were designed so as to eliminate a major portion of each gene in order to ensure the inactivation of its product. Two deletion alleles of *hoxK* were generated. Plasmid pCH497 was cut with *Nae*I and religated, producing plasmid pCH498. A second derivative lacking 36 bp of the 5′ region corresponding to leader sequences was obtained by ligating a 490-bp *Fsp*I-*Nae*I fragment of pCH311 into *Sca*I (partial)-*Eco*RV-cut pCH497. The resulting plasmid was designated pCH500. Plasmids pCH182, pCH460, pCH409, pCH460, pCH462, and pCH466 were used to generate the deletions in *hoxG*, *hoxZ*, *hoxM*, *hoxL*, *hoxO*, *hoxQ*, and *hoxV*. Plasmid pCH182 was cut with *Nde*I, end polished, recut with *Bsa*BI, and ligated, yielding plasmid pCH423. Plasmid pCH409 was cut with *Sal*I, end polished, cut with *Eco*RI, and ligated to a 1,176-bp *Eco*RI-*Sca*I fragment from a separate digest of the same parental plasmid. This procedure gave rise to plasmid pCH410. Digestion of plasmid pCH466 with *Nae*I and subsequent religation yielded pCH467. Plasmid pCH305 was cut with *Nco*I, end polished, cut with *Eco*RV, and religated. The resulting plasmid was designated pCH429.

Deletions in *hoxZ* and *hoxL* were obtained by amplification of appropriate template plasmids with mutagenic primers. One primer of each pair consisted of sequences flanking the desired deletion and thus contained the fusion joint (indicated below by hyphenation). Amplification of the *hoxZ* region in pCH460 with primer pair 5′-ATCTTGCGCACGCTGCATTCG-3′ and 5′-TTGCATTG CGCATCAGTCCTT-CGCCTCATAAACATAAGTGG-3′ produced a 274-bp fragment encompassing a 621-bp deletion. This fragment was cut with *Fsp*I and ligated into *Fsp*I-cut pCH460 in place of the wild-type sequence, producing plasmid pCH461. Similarly, amplification of the *hoxL* region in pCH462 with primer pair 5′-CGTATTCGTCCCAGTCGCGCATGCCGGCG-3′ and 5′-CGG AGAGTCTCGAG-CGATGCCACGCTGGATATGC-3′ and introduction of the resulting 520-bp *Sph*I-*Xho*I-cut product into *Sph*I-*Xho*I-cut pCH462 gave plasmid pCH463. For construction of a deletion in *hoxQ*, a synthetic adapter was prepared by hybridization of oligonucleotides 5′-AATTCATTTCCCATTCCG GTCGTGCTGGCCTGCG-3′ and 5′-AGGCCAGCACGACCGGAATGGGA AATG-3′. This adapter was used to link the ends of *Eco*RI-*Sfi*I-cut pCH469, yielding plasmid pCH471. Each of the modified sequences was transferred to pLO1 or pLO2 for reintroduction into *A. eutrophus* (24).

Deletion alleles of *hoxR* and *hoxT* were constructed from pLO1 derivatives harboring the corresponding wild-type sequences. Plasmid pCH425 was cut with *Bst*BI and *Rsr*II, end polished, and religated, producing plasmid pCH426. Plasmid pCH427 was cut with *Sal*I, Klenow treated, cut with *Eco*RV, and religated, yielding pCH428. All fusion joints were verified by sequencing. PCR products used for cloning were sequenced in their entireties. Sequences were determined by the method of Sanger et al. (34) with Sequenase 2.0 (United States Biochemical) and ^{35}S-dATP.

Media and growth conditions. Strains of *A. eutrophus* were grown in Luria broth medium containing 0.25% (wt/vol) sodium chloride (LSLB) or in a mineral salts medium (37). Synthetic media for heterotrophic growth contained 0.4% (wt/vol) fructose or a mixture of 0.2% (wt/vol) fructose and 0.2% (wt/vol) glycerol (FGN). Lithoautotrophically grown cells were cultivated in mineral salts medium under an atmosphere of hydrogen, carbon dioxide, and oxygen (8:1:1, vol/vol/vol). Sucrose-resistant segregants of *sacB*-harboring strains were selected on LSLB plates containing 15% (wt/vol) sucrose (24). Strains of *E. coli* were grown in Luria broth medium (30). Solid media contained 1.5% (wt/vol) agar. Antibiotics for *A. eutrophus* were used at the following concentrations: kanamycin, 350 μg/ml; and tetracycline, 15 μg/ml. Antibiotics for *E. coli* were used at the following concentrations: kanamycin, 25 μg/ml; tetracycline, 15 μg/ml; and ampicillin, 100 μg/ml.

Gene replacement. Modified *hox* sequences were reintroduced into *A. eutrophus* via conjugation with suicide vectors pLO1 and pLO2 (24). The allelic exchange procedure took advantage of the conditionally lethal *sacB* gene (14). The resultant sucrose-resistant isolates were screened for the presence of the desired mutation by amplification of the respective target sites. One milliliter of a fresh overnight culture was harvested, concentrated twofold in distilled water, and boiled for 5 min. Ten microliters of this lysate was used for a standard PCR amplification reaction. Deletion-carrying isolates were identified on the basis of the altered electrophoretic mobilities of the amplification products. All mutants were examined by Southern blot analysis in order to exclude sequence rearrangements adjacent to the deletion sites (40).

Western immunoblot analysis. Cells were homogenized in a French pressure cell, and the resulting crude extract was separated into soluble and membrane fractions as described previously (13). Proteins were resolved by electrophoresis in 10% polyacrylamide–sodium dodecyl sulfate (SDS) gels (21). Western immunoblot analysis was performed according to a standard protocol (42) with anti-HoxG serum at a dilution of 1:5,000.

Labeling with ^{63}nickel chloride. To monitor nickel incorporation into hydrogenase proteins, cells were grown in FGN in the presence of 150 nM $^{63}NiCl_2$ (6.38 mCi/ml; Amersham-Buchler). The membrane fraction was solubilized with Triton X-114 (final concentration, 2%) in the cold (4°C) for 45 min (2). After an incubation for 2 min at 37°C, the extract was centrifuged for 15 min at 10,000 × *g* and 20°C. The resulting supernatant is referred to below as solubilized membrane fraction. Solubilized membrane proteins were resolved by native electrophoresis in 4 to 15% acrylamide gradient gels by the method of Lambin and Fine (22). Gels were run in a continuous buffer system consisting of 90 mM Tris, 80 mM borate, and 2.5 mM EDTA (pH 8.3) at 200 V and 4°C for 2,500 V · h. After electrophoresis, the gels were soaked for 15 min in Amplify (Amersham-Buchler), dried under vacuum, and subjected to autoradiography.

Enzyme assays. Hydrogenase assays were performed with cells grown lithoautotrophically or heterotrophically on FGN as described previously (13). SH (hydrogen:NAD^+ oxidoreductase; EC 1.12.1.2) activity was determined by monitoring H_2-dependent NAD reduction in the soluble fraction (38). MBH (hydrogen:acceptor oxidoreductase; EC 1.18.99.1) activity was measured in the membrane fraction with methylene blue being used as the electron acceptor (36). For in-gel chromogenic detection of hydrogenase activity, soluble extracts and Triton X-114-treated membrane extracts were resolved by native polyacrylamide gel electrophoresis (PAGE). The gels were subsequently incubated in 50 mM potassium phosphate buffer (pH 5.5) that was H_2 saturated and that contained 0.09 mM phenazine methosulfate (PMS) and 0.06 mM nitroblue tetrazolium under an atmosphere of H_2 at 30°C.

RESULTS

In-frame deletions in the MBH region. To investigate the roles of the MBH accessory genes *hoxZ*, *hoxM*, *hoxL*, *hoxO*, *hoxQ*, *hoxR*, *hoxT*, and *hoxV* in H_2 oxidation, we introduced in-frame deletions into each gene via allelic exchange as described in Materials and Methods. We also generated isogenic *hoxK* and *hoxG* deletion mutants by the same procedure to compare the accessory gene mutants with strains carrying well-defined mutations in the MBH structural genes. One of the two *hoxK* deletion derivatives (HF403) harbored a lesion in the segment of the gene corresponding to the mature protein; the other (HF404) harbored a lesion in the leader-determining sequence (Fig. 1). We first tested the mutants for autotrophic growth on H_2. All of the mutant strains grew at wild-type rates (doubling time, 4.1 h) under these conditions. Even strain HF359, which carries an extensive deletion in the gene for HoxG, grew at a normal rate. This observation was not surprising in light of previous findings for MBH null mutants (17). Under laboratory conditions, the contribution of the MBH to autotrophic growth is apparent only in SH^- mutants. In these strains, MBH-catalyzed H_2 oxidation supports growth at low rates. Double mutants harboring a deletion in the structural genes or MBH accessory genes in addition to a lesion in the SH operon completely failed to grow autotrophically on H_2 (data not shown). We next examined the mutant strains for MBH activity. Table 2 gives the H_2-dependent rate of methylene blue reduction present in the membrane fraction. Although the absolute values for a given strain differed under lithoautotrophic and heterotrophic conditions, the ratio of mutant and wild-type activities under both growth conditions was the same in all cases. Therefore, a single value is given (Table 2). With the exception of the *hoxT* mutant (HF363), all of the other strains contained dramatically reduced levels of MBH activity. The major group of mutants, *hoxG*Δ, *hoxK*Δ, *hoxK*leaderΔ, *hoxZ*Δ, *hoxM*Δ, *hoxO*Δ, and *hoxQ*Δ mutants (HF359, HF403, HF404, HF405, HF345, HF407, and HF408), was totally devoid of MBH activity. Three isolates, *hoxL*Δ, *hoxR*Δ, and *hoxV*Δ mutants (HF406, HF361, and HF365), contained 10 to 30% of the wild-type activity. The slight reduction in MBH activity in the *hoxT* mutant was surprising in light of the observation that the mutation prevented lithoautotrophic growth in the SH^- background. Thus, the product of *hoxT* may be involved in H_2-dependent electron transport reactions.

None of the mutants of this collection showed significant differences in SH activity, ruling out the possibility that the mutations had a pleiotropic effect on the activity of both hydrogenases of *A. eutrophus*. Introduction of plasmid-borne copies of each of the 10 genes (Fig. 1 [hatched boxes]) under the control of the *lac* promoter complemented the corresponding mutation, indicating that the mutant phenotypes were in fact due to the inactivation of the respective gene products and not to polar effects on downstream genes.

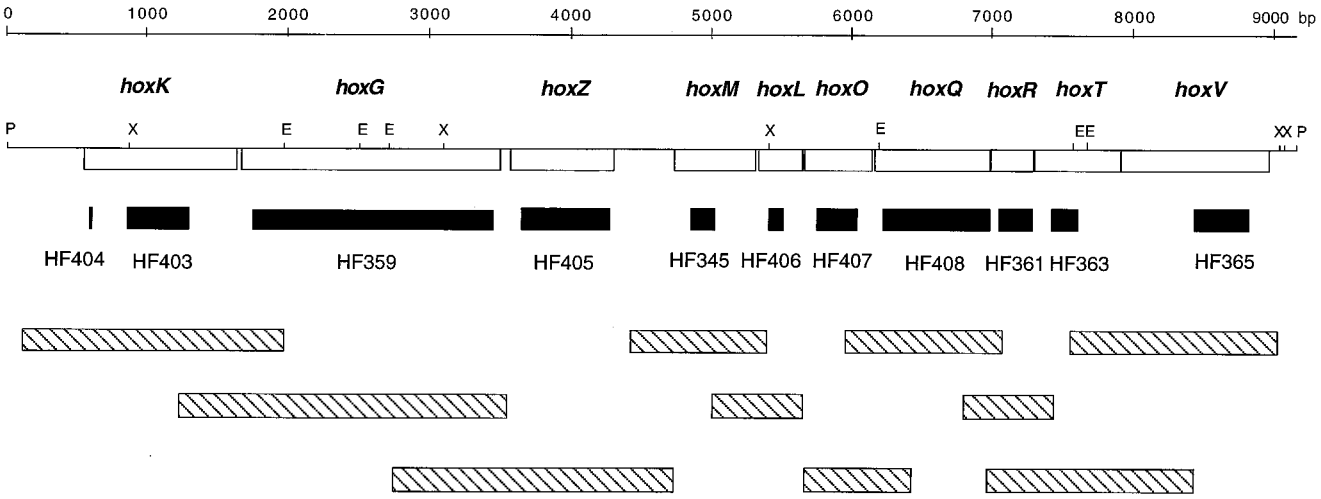

FIG. 1. Genetic map of the MBH region of *A. eutrophus* H16. A simplified restriction map with genes indicated as open boxes is given in the upper part of the figure. Solid bars represent the positions and extents of in-frame deletions. The designations of the respective mutant strains are given below each bar. Fragments subcloned in broad-host-range plasmid pGE151 for complementation tests are represented as hatched bars. The scale is in base pairs. Restriction sites: E, *Eco*RI; P, *Pst*I; X, *Xho*I.

Cellular distribution of the MBH protein. To investigate the molecular basis of the alterations in MBH activity, we screened membrane and soluble fractions of the various mutants for the presence of MBH protein. For these immunochemical experiments, we used an antiserum directed against HoxG of the MBH. This subunit harbors the nickel-containing active site of the enzyme. Figure 2A demonstrates the results obtained with membrane extracts. The wild type (Fig. 2A, lane 1) showed a strong signal below 69 kDa corresponding to HoxG. The weakly stained band in the lower part of the gel, visible in all lanes, is attributable to a nonspecific cross-reaction. The mutants lacking MBH activity altogether were nearly devoid of immunoreactive HoxG. Significantly reduced amounts of cross-reactive material were detectable in mutants with intermediate levels of MBH activity. Membrane extracts from the *hoxZ*, *hoxM*, *hoxL*, and *hoxO* mutants (Fig. 2A, lanes 5 to 8) clearly contained two forms of HoxG differing in electrophoretic mobility. While the *hoxZ* and *hoxL* extracts contained a fast-migrating form, the *hoxM* and *hoxO* extracts revealed a slowly moving species referred to as the precursor.

The reduced amount of immunologically detectable HoxG present in the membranes of the mutant cells might be the result of low gene expression, decreased stability of the MBH protein, and/or perturbation of the events leading to membrane attachment of the enzyme. To answer this question, we screened the soluble fraction of the mutants for HoxG. As can be seen from Fig. 2B, all of the mutants, with the exception of the *hoxG*Δ strain (lane 2), contained cross-reacting material. Furthermore, most of the soluble HoxG was present in the unprocessed form. The analysis of the *hoxZ* mutant which is lacking a membrane-bound cytochrome *b*-like protein (20) showed that both forms of HoxG were present in approximately equal amounts (Fig. 2B, lane 5). This result points to a defect in the process of membrane attachment.

Catalytic MBH activity in the soluble and membrane fractions. The immunoblotting experiments described above showed the distribution of the mature form of precursor HoxG in the membrane and soluble cell extracts. This observation prompted us to examine the catalytic MBH activity in both cell

TABLE 2. MBH activity in the membrane fraction

Strain	Genotype	Activity (%)[a]
H16	Wild type	100
HF404	*hoxK*Δleader	0
HF403	*hoxK*Δ	0
HF359	*hoxG*Δ	0
HF405	*hoxZ*Δ	0
HF345	*hoxM*Δ	0
HF406	*hoxL*Δ	10
HF407	*hoxO*Δ	0
HF408	*hoxQ*Δ	0
HF361	*hoxR*Δ	30
HF363	*hoxT*Δ	90
HF365	*hoxV*Δ	30

[a] H_2-dependent methylene blue reduction in heterotrophically (fructose-glycerol) and autotrophically (H_2-O_2-CO_2) grown cells. The MBH activity of the wild type is taken as 100%. Values are the averages of three independent experiments conducted under both conditions. Corrections were not necessary, since the *hoxG* deletion strain was devoid of background activity.

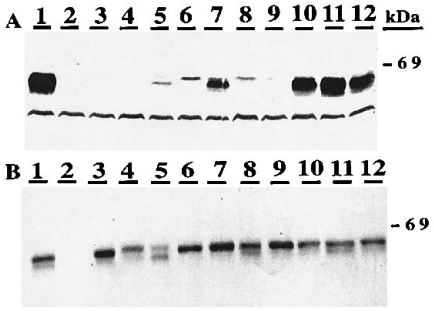

FIG. 2. Western immunoblot analysis of *A. eutrophus* H16 and mutant derivatives. Cells were grown in FGN. Membrane (A) and soluble (B) fractions were prepared from crude homogenates. Protein samples (25 μg each) were separated in SDS–10% PAGE gels. Proteins were subsequently transferred to nitrocellulose membranes by electroblotting. Blots were developed with a polyclonal antiserum directed against HoxG (diluted 1:5,000) and a goat anti-rabbit alkaline phosphatase conjugate. Lane 1, H16; lane 2, HF359 (*hoxG*Δ); lane 3, HF404 (*hoxK*Δleader); lane 4, HF403 (*hoxK*Δ); lane 5, HF405 (*hoxZ*Δ); lane 6, HF345 (*hoxM*Δ); lane 7, HF406 (*hoxL*Δ); lane 8, HF407 (*hoxO*Δ); lane 9, HF408 (*hoxQ*Δ); lane 10, HF361 (*hoxR*Δ); lane 11, HF363 (*hoxT*Δ); lane 12, HF365 (*hoxV*Δ). The position of a 69-kDa marker protein is given at the right.

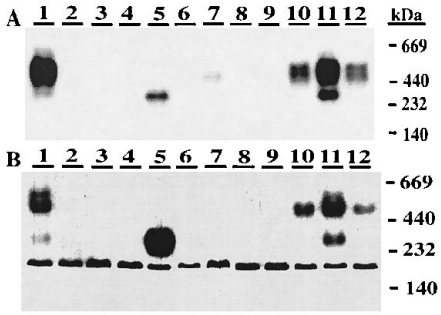

FIG. 3. MBH activity staining. Cells were grown in FGN. Triton X-114 solubilized membrane (A) and soluble (B) proteins were prepared from crude homogenates. Protein samples (A, 15 μg each; B, 150 μg each) were separated in 4 to 15% native PAGE gels. Subsequently, the gels were soaked in 50 mM potassium phosphate buffer (pH 5.5) that was saturated with H_2 and that contained 0.09 mM PMS and 0.06 mM nitroblue tetrazolium under a hydrogen atmosphere. Lane 1, H16; lane 2, HF359 (*hoxG*Δ); lane 3, HF404 (*hoxK*Δleader); lane 4, HF403 (*hoxK*Δ); lane 5, HF405 (*hoxZ*Δ); lane 6, HF345 (*hoxM*Δ); lane 7, HF406 (*hoxL*Δ); lane 8, HF407 (*hoxO*Δ); lane 9, HF408 (*hoxQ*Δ); lane 10, HF361 (*hoxR*Δ); lane 11, HF363 (*hoxT*Δ); lane 12, HF365 (*hoxV*Δ). The positions of marker proteins are given at the right in kilodaltons.

fractions. To avoid interference with the SH enzyme, we separated the soluble proteins in native PAGE gels and performed in-gel hydrogenase activity staining with PMS being used as an artificial electron acceptor. For purposes of comparison, the same analysis was carried out with solubilized membrane proteins. The results of the latter experiment (Fig. 3A) are in good agreement with the MBH activities determined by H_2-dependent methylene blue reduction (Table 2). Strong staining was observed for the wild type and the *hoxT* mutant (Fig. 3A, lanes 1 and 11). Intermediate activity was detectable for the *hoxR* and *hoxV* mutants (Fig. 3A, lanes 10 and 12), and traces of activity were identified for the *hoxL* mutant (lane 7). Not surprisingly, no staining reaction was found for the *hoxG*, *hoxK*, *hoxM*, *hoxO*, and *hoxQ* mutants (Fig. 3A, lanes 2 to 4, 6, 8, and 9). Interestingly, membranes from the *hoxZ* mutant contained PMS-reducing activity (Fig. 3A, lane 5), although no H_2-dependent methylene blue reduction was detectable in this strain (Table 2). This discrepancy may be explained by different assay conditions. Moreover, the position of the band was different and correlated with a minor species also present in the *hoxT* mutant (Fig. 3A, lane 11), indicating a different conformer.

Activity staining of the proteins in the soluble extracts revealed several prominent bands; the fast-moving species is nonspecific and did not correlate with hydrogenase activity (Fig. 3B). The extract from the wild type and the *hoxT* mutant yielded three PMS-reducing species (Fig. 3B, lanes 1 and 11). A single band was visible in the soluble extracts from the *hoxR* and *hoxV* mutants (Fig. 3B, lanes 10 and 12). As was expected, no PMS-reducing activity was detectable in the soluble fractions from the *hoxG*, *hoxK*, *hoxM*, *hoxL*, *hoxO*, and *hoxQ* mutants (Fig. 3B, lanes 2 to 4 and 6 to 9), which is consistent with the lack of methylene blue-reducing activity (Table 2). On the other hand, the *hoxZ* mutant (Fig. 3B, lane 5) showed a strong PMS-reducing activity, and again, a change in mobility indicated a different conformer.

Incorporation of ^{63}Ni into MBH. Previous studies in our laboratory showed that the incorporation of nickel into the MBH is intimately connected with the modification of HoxG and the acquisition of catalytic activity (7). To monitor nickel incorporation into the MBH, cells were grown in FGN in the presence of 150 nM $^{63}NiCl_2$ and soluble and membrane fractions were prepared. After solubilization of the membrane proteins with Triton X-114, the labeled proteins were separated in native PAGE gels. Figure 4A documents the incorporation of ^{63}Ni into membrane proteins. A single prominent signal was apparent in the sample from the wild-type strain (Fig. 4A, lane 1). The absence of this band in the *hoxG* deletion mutant (Fig. 4A, lane 3) and its coincidence with the position of the PMS-reducing activity in activity-stained gels identified the labeled species as the MBH. Interestingly, the MBH signal was more intense in a mutant (*hoxH*Δ) from which the nickel-containing subunit of the SH had been deleted, suggesting that the two enzymes compete for the available nickel (Fig. 4A, lane 2). No label was detectable in the membranes from the *hoxK*, *hoxM*, *hoxO*, and *hoxQ* deletion strains, which are all devoid of methylene blue-reducing activity (Fig. 4A, lanes 4, 5, 7, 9, and 10). The various amounts of labeled MBH which were found in the *hoxL*, *hoxR*, *hoxT*, and *hoxV* mutants correlated with the MBH activity shown in Table 2. The *hoxZ* mutant (Fig. 4A, lane 6) which was devoid of methylene blue-reducing activity (Table 2) but which revealed H_2-dependent PMS reduction (Fig. 3A, lane 5) showed a ^{63}Ni signal only after long exposure of the autoradiogram (data not shown).

The corresponding autoradiogram for the soluble extracts (Fig. 4B) revealed a complex pattern of labeled proteins, several of which have been assigned to the SH by previous work (7). Comparison of the patterns for the wild-type and *hoxG* deletion strains (Fig. 4B, lanes 1 and 3) pointed out a set of bands attributable to the MBH. Here again, labeling of the MBH was more intense in the strain from which *hoxH* had been deleted (Fig. 4B, lane 2). Two major signals corresponding to a slowly and a slightly faster migrating protein were apparent. These signals probably correspond to different aggregates containing HoxG. These bands were similar in the various mutant strains, with the exception of the *hoxM* mutant (Fig. 4B, lane 7), which was completely inactive in HoxG mat-

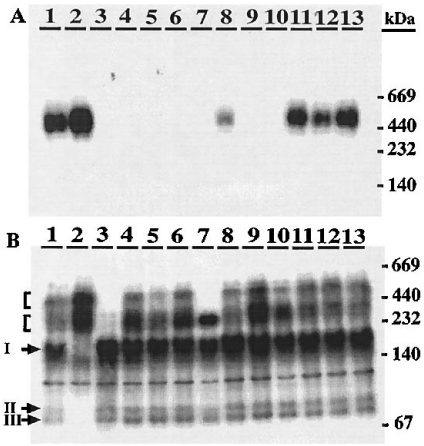

FIG. 4. ^{63}Ni incorporation in vivo. Cells were grown in FGN in the presence of 150 nM $^{63}NiCl_2$. Triton X-114-solubilized membrane (A) and soluble (B) proteins were prepared from crude homogenates and separated in 4 to 15% native PAGE gels. The gels were subsequently dried and autoradiographed. Lane 1, H16; lane 2, HF388 (*hoxH*Δ); lane 3, HF359 (*hoxG*Δ); lane 4, HF404 (*hoxK*Δleader); lane 5, HF403 (*hoxK*Δ); lane 6, HF405 (*hoxZ*Δ); lane 7, HF345 (*hoxM*Δ); lane 8, HF406 (*hoxL*Δ); lane 9, HF407 (*hoxO*Δ); lane 10, HF408 (*hoxQ*Δ); lane 11, HF361 (*hoxR*Δ); lane 12, HF363 (*hoxT*Δ); lane 13, HF365 (*hoxV*Δ). Arrows indicate ^{63}Ni-labeled SH polypeptides. I, tetrameric holoenzyme; II, HoxH precursor; III, mature HoxH. Brackets mark ^{63}Ni-labeled MBH proteins or MBH-containing complexes. The positions of protein standards are given at the right in kilodaltons.

uration (Fig. 2, lanes 6). The slowly migrating protein was absent in the *hoxM* mutant, whereas the second signal was enhanced, suggesting that the latter represents a maturation intermediate. The intensity of the bands from the wild-type and mutant strains is to some extent inversely correlated with the intensity of the label in the corresponding membrane fractions. This result is compatible with the assumption that a block in the process of membrane attachment leads to the accumulation of soluble proteins.

DISCUSSION

We carried out a systematic genetic analysis of the *A. eutrophus* MBH locus. Our findings show that all accessory genes are essential for MBH-mediated lithoautotrophic growth. Homologous gene clusters in other H_2-oxidizing bacteria, including *E. coli* (27–29), *Rhodobacter capsulatus* (6, 23), *Rhizobium leguminosarum* (15, 16, 32), *Azotobacter vinelandii* (4, 5, 25, 26), and *Azotobacter chroococcum* (9, 11), have been identified and studied. Most of these studies relied on polar mutations, which prevented the unambiguous assignment of phenotypes, thereby critically limiting the interpretability of the biochemical and immunological data. Other investigations were based on complementation by sequences carried on high-copy plasmids, which can produce phenotypical artifacts because of an imbalance in gene products.

The MBH accessory mutants described in this report can be grouped in two major classes on the basis of MBH activity. Class I consists of mutants with defects in genes *hoxM*, *hoxO*, and *hoxQ*, which were totally devoid of MBH activity and thus resembled the structural gene mutants. Class II mutants contained different levels of residual MBH activity. The *hoxZ*, *hoxL*, *hoxR*, *hoxT*, and *hoxV* mutants belonged to this group. Additional analyses revealed that the two groups were in fact heterogeneous.

The *hoxM* deletion strain was the only mutant in our collection which contained no immunologically detectable HoxG subunit in the mature form. Thus, the defect in *hoxM* blocked modification of HoxG completely and impaired the association of MBH with the membrane but did not block it completely. Hence, only a small fraction of HoxG was identified in the membrane of the *hoxM* mutant, confirming previous observations with insertion mutants (20). We also found an abnormal pattern of ^{63}Ni labeling in this mutant. Thus, the *hoxM* gene product could mediate modification of HoxG and/or a key step in metal center assembly. We can nevertheless exclude the possibility that the *hoxM* product affects the process of membrane attachment per se. Furthermore, *hoxM* is a member of a family of homologous genes which includes the *hoxM* genes of *A. vinelandii* (25), the *hupD* genes of *R. capsulatus* (6), *R. leguminosarum* (16), and *Bradyrhizobium japonicum* (45), and the *hyaD* (28), *hybD* (27), and *hycI* (33) genes of *E. coli*. The *E. coli hycI* gene product has been purified, and in vitro studies with the purified protein showed that it mediates C-terminal processing of the HycE precursor (33). This result suggests a similar function for the other members of the family, including *A. eutrophus* HoxM, and implies that the effects on ^{63}Ni labeling and membrane association in the *hoxM* mutant are secondary. The *A. eutrophus* HoxW protein belongs to the same family. HoxW specifically mediates proteolytic processing of the large subunit of the SH (41).

In contrast to the mutation in *hoxM*, defects in *hoxO* and *hoxQ* impair HoxG modification but do not block it completely and do not significantly alter the pattern of ^{63}Ni labeling. In the *hoxQ* mutant, the amount of processed HoxG is drastically reduced, suggesting that the *hoxQ* gene product is important although not essential for the processing of HoxG. The *hoxO* mutant, on the other hand, contains normal levels of processed HoxG in the soluble extract. These results indicate that there are maturation reactions aside from C-terminal proteolysis of HoxG and incorporation of Ni which are essential for the formation of active MBH. These processes could involve small subunit HoxK.

Class II mutants produce MBH activity, albeit at more or less reduced levels. The *hoxT* mutant contained almost wild-type-like, membrane-associated MBH activity. It is therefore remarkable that a double mutant bearing a second site deletion in a structural gene of the SH did not grow lithoautotrophically. The *hoxT* gene product does not seem to be involved in MBH maturation. We considered the possibility that the cysteine-rich, 20-kDa HoxT protein plays a role in H_2-dependent electron transport. The effects of the *hoxR* and *hoxV* mutations on MBH were more pronounced, since MBH activity was reduced to one-third of the wild-type level. While the distribution of immunoreactive HoxG and incorporation of ^{63}Ni were indistinguishable from those of the wild-type situation, only one of the three PMS-reducing species was present in the soluble extract of the mutants. Sequence comparisons showed without a doubt that the *hoxR* gene product is a rubredoxin (20). At present, we have no clues about the role of such a protein in the synthesis of catalytically active MBH. The absence of a homologous gene in the hydrogenase operons of *E. coli*, which produces hydrogenase only under anaerobic conditions, may be an indication that the HoxR homologs of the aerobic H_2 oxidizers serve to protect hydrogenase against O_2. An *hoxV* homolog has been identified in the MBH gene cluster of *R. leguminosarum* (32). A role in the assembly of the Ni metallocenter was postulated for this gene product, but no experimental evidence is available (18). The pattern of ^{63}Ni labeling found for the *A. eutrophus hoxV* mutant was indistinguishable from that of the wild type. Beside Ni, a second metal, probably Fe, was found to be present in the catalytic center (47), pointing to a complex process of metollocenter assembly. Whatever the role of the *hoxV* product is, it is obviously nonessential.

MBH activity of the *hoxL* mutant was reduced to 10%, pointing to an important function of the *hoxL* gene product. The *hoxL* gene is homologous to another hydrogenase-related gene of *A. eutrophus*, *hypC*, which shows features typical of a ferredoxin-like protein (20). While a mutation in *hypC* blocks ^{63}Ni incorporation and C-terminal processing of both MBH and SH (7), a mutation in *hoxL* affected maturation of MBH only. Thus, the phenotypes of the *hoxL* and *hypC* mutants are clearly different, pointing to a specialization of the gene products.

The phenotype of the *hoxZ* mutant sets this strain appart from the rest. Although both the soluble and membrane fractions of the *hoxZ* mutant contained PMS-reducing activity, the preponderance of this activity was soluble. Both HoxG processing and Ni labeling appeared to proceed normally. *hoxZ* belongs to a family of genes which accompany the hydrogenase structural genes in various aerobic H_2 oxidizers (12). The deduced sequences of the corresponding gene products predict that they are integral membrane proteins which have certain features typical of *b*-type cytochromes (1, 8, 20). Four biological functions have been discussed for these proteins (35): (i) coupling of the hydrogenase to an electron transport chain, (ii) reductive activation of the hydrogenase enzyme, (iii) anchoring of hydrogenase in the membrane, and (iv) stabilization of the hydrogenase enzyme. The results presented here are compatible with the first and third functions but argue against the second and fourth. The loss of a coupling function could ex-

plain the fact that the *hoxZ* mutant was unable to grow lithoautotrophically, despite the presence of massive amounts of PMS-reducing activity. This activity was found predominately in the soluble fraction, and only a minor amount was associated with the membrane. Our results parallel and extend the findings reported for homologous gene products of other H_2-oxidizing bacteria. The product of *hydC*, the *hoxZ* homolog of *Wolinella succinogenes*, is required for the H_2-dependent reduction of 2,3-dimethyl-1,4-naphthoquinone, an analog of the physiological electron acceptor menaquinone, by hydrogenase. The hydrogenase dimer is not incorporated into liposomes in the absence of HydC (8). A defect in the *hoxZ* gene of *A. vinelandii* led to the uncoupling of H_2 oxidation and O_2 reduction (35).

Two *hoxK* mutants were included in these studies as controls. The results obtained with these mutants provide some important insights into MBH maturation. Strain HF404 had 36 bp of the 129-bp leader-determining sequence deleted. This deletion should eliminate the critical part of the leader peptide containing the conserved hydrogenase leader motif (R-R-X-X-F-X-K) and thereby block translocation of HoxK. A special translocation process is probably required for the positioning of the MBH enzyme on the membrane (31, 44). Our findings are compatible with this notion. Membranes prepared from leader deletion mutant HF404 were devoid of MBH activity. Interestingly, immunoreactive HoxG was also absent from the membrane fraction. Thus, it appears that translocatable HoxK is essential for attachment of HoxG to the membrane.

The analyses reported here delineate the roles of the eight genes in MBH maturation, but we are still far from an understanding of this complex process. A careful investigation of the effects of the various mutations on the HoxK subunit is required. Much work will be needed to determine the precise order of events in MBH maturation. Another intriguing question concerns the structural basis for the attachment of the hydrogenase enzyme to the membrane. The putative transmembrane helix at the C terminus of HoxK is not sufficient for membrane attachment, but association with HoxZ could contribute to the anchoring of the enzyme in the membrane. A recent immunocytochemical investigation demonstrated that part if not all of the MBH is exposed to the periplasm (10). On the basis of this finding and our observations with the *hoxZ* mutant, we postulate that the MBH holoenzyme is located entirely on the periplasmic face of the membrane. Experiments are now under way to examine this hypothesis. The *hoxZ* mutant provides an excellent tool to test this experimentally.

ACKNOWLEDGMENTS

We are grateful to A. Strack for excellent technical assistance.

This work was supported by grants from the Bundesministerium für Wissenschaft und Forschung and Fonds der Chemischen Industrie.

REFERENCES

1. **Berks, B. C., M. D. Page, D. J. Richardson, A. Reilly, A. Cavill, F. Outen, and S. Ferguson.** 1994. Sequence analysis of subunits of the membrane-bound nitrate reductase from a denitrifying bacterium: the integral membrane subunit provides a prototype for the dihaem electron-carrying arm of a redox loop. Mol. Microbiol. **15:**319–331.
2. **Bordier, C.** 1981. Phase separation of integral membrane proteins in Triton X-114 solution. J. Biol. Chem. **256:**1604–1607.
3. **Chang, A. C. Y., and S. N. Cohen.** 1978. Construction and characterization of amplifiable multicopy DNA cloning vehicles derived from the P15A cryptic miniplasmid. J. Bacteriol. **134:**1141–1156.
4. **Chen, J. C., and L. E. Mortenson.** 1992. Two open reading frames (ORFs) identified near the hydrogenase structural genes in *Azotobacter vinelandii*, the first ORF may encode for a polypeptide similar to rubredoxins. Biochim. Biophys. Acta **1131:**122–124.
5. **Chen, J. C., and L. E. Mortenson.** 1992. Identification of six open reading frames from a region of the *Azotobacter vinelandii* genome. Biochim. Biophys. Acta **1131:**199–202.
6. **Colbeau, A., P. Richaud, B. Toussaint, F. J. Caballero, C. Elster, C. Delphin, R. L. Smith, J. Chabert, and P. M. Vignais.** 1993. Organization of the genes necessary for hydrogenase expression in *Rhodobacter capsulatus*. Sequence analysis and identification of two *hyp* regulatory mutants. Mol. Microbiol. **8:**15–29.
7. **Dernedde, J., T. Eitinger, N. Patenge, and B. Friedrich.** 1996. *hyp* gene products in *Alcaligenes eutrophus* are part of a hydrogenase maturation system. Eur. J. Biochem. **235:**351–358.
8. **Dross, F., V. Geisler, R. Lenger, F. Theis, T. Kraft, F. Falkenholz, E. Kojro, A. Duchêne, D. Tripier, K. Juvenal, and A. Kröger.** 1992. The quinone-reactive Ni/Fe-hydrogenase of *Wolinella succinogenes*. Eur. J. Biochem. **206:** 93–102.
9. **Du, L., F. Stejskal, and K. H. Tibelius.** 1992. Characterization of two genes (*hupD* and *hupE*) required for hydrogenase activity in *Azotobacter chroococcum*. FEMS Microbiol. Lett. **96:**93–102.
10. **Eismann, K., K. Milejnek, D. Zipprich, M. Hoppert, H. Gerberding, and F. Mayer.** 1995. Antigenic determinants of the membrane-bound hydrogenase in *Alcaligenes eutrophus* are exposed toward the periplasm. J. Bacteriol. **177:**6309–6312.
11. **Ford, C. M., N. Garg, R. P. Garg, K. H. Tibelius, M. G. Yates, D. J. Arp, and L. C. Seefeldt.** 1990. The identification, characterization, sequencing and mutagenesis of the genes (*hupSL*) encoding the small and large subunits of the H_2-uptake hydrogenase of *Azotobacter chroococcum*. Mol. Microbiol. **4:**999–1008.
12. **Friedrich, B., and E. Schwartz.** 1993. Molecular biology of hydrogen utilization in aerobic chemolithotrophs. Annu. Rev. Microbiol. **47:**351–383.
13. **Friedrich, C. G., B. Friedrich, and B. Bowien.** 1981. Formation of enzymes of autotrophic metabolism during heterotrophic growth of *A. eutrophus*. J. Gen. Microbiol. **122:**69–78.
14. **Gay, P., D. Le Coq, M. Steinmetz, T. Berkelmann, and C. I. Kado.** 1985. Positive selection procedure for entrapment of insertion sequence elements in gram-negative bacteria. J. Bacteriol. **164:**918–921.
15. **Hidalgo, E., A. Leyva, and T. Ruiz-Argüeso.** 1990. Nucleotide sequence of the hydrogenase structural genes from *Rhizobium leguminosarum*. Plant Mol. Biol. **15:**367–370.
16. **Hidalgo, E., J. M. Palacios, J. Murillo, and T. Ruiz-Argüeso.** 1992. Nucleotide sequence and characterization of four additional genes of the hydrogenase structural operon from *Rhizobium leguminosarum* bv. viciae. J. Bacteriol. **174:**4130–4139.
17. **Hogrefe, C., D. Römermann, and B. Friedrich.** 1984. *Alcaligenes eutrophus* hydrogenase genes (*hox*). J. Bacteriol. **158:**43–48.
18. **Imperial, J., L. Rey, J. M. Palacios, and T. Ruiz-Argüeso.** 1993. HupK, a hydrogenase-ancillary protein from *Rhizobium leguminosarum*, shares structural motifs with the large subunit of [NiFe]hydrogenases and could be a scaffolding protein for hydrogenase metal cofactor assembly. Mol. Microbiol. **9:**1305–1306.
19. **Kortlüke, C., and B. Friedrich.** 1992. Maturation of membrane-bound hydrogenase of *Alcaligenes eutrophus* H16. J. Bacteriol. **174:**6290–6293.
20. **Kortlüke, C., K. Horstmann, E. Schwartz, M. Rohde, R. Binsack, and B. Friedrich.** 1992. A gene complex coding for the membrane-bound hydrogenase of *Alcaligenes eutrophus* H16. J. Bacteriol. **174:**6277–6289.
21. **Laemmli, U. K.** 1972. Cleavage of structural proteins during the assembly of the head of bacteriophage T4. Nature (London) **227:**680–685.
22. **Lambin, P., and J. M. Fine.** 1979. Molecular weight estimation of proteins by electrophoresis in linear polyacrylamide gradient gels in absence of denaturing agents. Anal. Biochem. **98:**160–168.
23. **Leclerc, M., A. Colbeau, B. Cauvin, and P. M. Vignais.** 1988. Cloning and sequencing of the genes encoding the large and the small subunits of the H_2 uptake hydrogenase (*hup*) of *Rhodobacter capsulatus*. Mol. Gen. Genet. **214:**97–107. (Erratum, **215:**368, 1989.)
24. **Lenz, O., E. Schwartz, J. Dernedde, M. Eitinger, and B. Friedrich.** 1994. The *Alcaligenes eutrophus* H16 *hoxX* gene participates in hydrogenase regulation. J. Bacteriol. **176:**4385–4393.
25. **Menon, A. L., L. E. Mortenson, and R. L. Robson.** 1992. Nucleotide sequences and genetic analysis of hydrogen oxidation (*hox*) genes in *Azotobacter vinelandii*. J. Bacteriol. **174:**4549–4557.
26. **Menon, A. L., L. W. Stultz, R. L. Robson, and L. E. Mortenson.** 1990. Cloning, sequencing and characterization of the [NiFe]hydrogenase-encoding structural genes (*hoxK* and *hoxG*) from *Azotobacter vinelandii*. Gene **96:**67–74.
27. **Menon, N. K., C. Y. Chatelus, M. Dervartanian, J. C. Wendt, K. T. Shanmugam, H. D. Peck, Jr., and A. E. Przybyla.** 1994. Cloning, sequencing, and mutational analysis of the *hyb* operon encoding *Escherichia coli* hydrogenase 2. J. Bacteriol. **176:**4416–4423.
28. **Menon, N. K., J. Robbins, H. D. Peck, Jr., C. Y. Chatelus, E.-S. Choi, and A. E. Przybyla.** 1990. Cloning and sequencing of a putative *Escherichia coli* [NiFe] hydrogenase-1 operon containing six open reading frames. J. Bacteriol. **172:**1969–1977.
29. **Menon, N. K., J. Robbins, J. C. Wendt, K. T. Shanmugam, and A. E. Przybyla.** 1991. Mutational analysis and characterization of the *Escherichia coli hya* operon, which encodes [NiFe] hydrogenase 1. J. Bacteriol. **173:**4851–4861.

30. **Miller, J. H.** 1972. Experiments in molecular genetics. Cold Spring Harbor Laboratory, Cold Spring Harbor, N.Y.
31. **Nivière, V., S. Wong, and G. Voordouw.** 1992. Site-directed mutagenesis of the hydrogenase signal peptide consensus box prevents export of a β-lactamase fusion protein. J. Gen. Microbiol. **138:**2173–2183.
32. **Rey, L., E. Hidalgo, J. M. Palacios, and T. Ruiz-Argüeso.** 1992. Nucleotide sequence and organization of an H_2-uptake gene cluster from *Rhizobium leguminosarum* bv. *viciae* containing a rubredoxin-like gene and four additional open reading frames. J. Mol. Biol. **228:**998–1002.
33. **Rossmann, R., T. Maier, F. Lottspeich, and A. Böck.** 1995. Characterization of a protease from *Escherichia coli* involved in hydrogenase maturation. Eur. J. Biochem. **227:**545–550.
34. **Sanger, F., S. Nicklen, and A. R. Coulson.** 1977. DNA sequencing with chain-terminating inhibitors. Proc. Natl. Acad. Sci. USA **74:**5463–5467.
35. **Sayavedra-Soto, L., and D. J. Arp.** 1992. The *hoxZ* gene of the *Azotobacter vinelandii* hydrogenase operon is required for activation of hydrogenase. J. Bacteriol. **174:**5295–5301.
36. **Schink, B., and H. G. Schlegel.** 1979. The membrane-bound hydrogenase of *Alcaligenes eutrophus*. Solubilization, purification and biochemical properties. Biochim. Biophys. Acta **567:**315–324.
37. **Schlegel, H. G., H. Kaltwasser, and G. Gottschalk.** 1961. Ein Submersverfahren zur Kultur wasserstoffoxidierender Bakterien: Wachstumsphysiologische Untersuchungen. Arch. Mikrobiol. **38:**315–324.
38. **Schneider, K., and H. G. Schlegel.** 1976. Purification and properties of the soluble hydrogenase from *Alcaligenes eutrophus* H16. Biochim. Biophys. Acta **452:**66–80.
39. **Simon, R., U. Priefer, and A. Pühler.** 1983. A broad host range mobilization system for *in vivo* genetic engineering: transposon mutagenesis in gram-negative bacteria. Bio/Technology **1:**717–743.
40. **Southern, E. M.** 1975. Detection of specific sequences among DNA fragments separated by gel electrophoresis. J. Mol. Biol. **98:**503–517.
41. **Thiemermann, S., J. Dernedde, M. Bernhard, W. Schroeder, C. Massanz, and B. Friedrich.** 1996. Carboxyl-terminal processing of the cytoplasmic NAD-reducing hydrogenase of *Alcaligenes eutrophus* requires the *hoxW* gene product. J. Bacteriol. **178:**2368–2374.
42. **Towbin, H., T. Staehelin, and J. Gordon.** 1979. Electrophoretic transfer of proteins from polyacrylamide gels to nitrocellulose sheets: procedure and some applications. Proc. Natl. Acad. Sci. USA **76:**4350–4354.
43. **Tran-Betcke, A., U. Warnecke, C. Böcker, C. Zaborosch, and B. Friedrich.** 1990. Cloning and nucleotide sequences of the genes for the subunits of NAD-reducing hydrogenase of *Alcaligenes eutrophus* H16. J. Bacteriol. **172:** 2920–2929.
44. **Van Dongen, W., W. Hagen, W. van den Berg, and C. Veeger.** 1988. Evidence for an unusual mechanism of membrane translocation of the periplasmic hydrogenase of *Desulfovibrio vulgaris* (Hildenborough), as derived from expression in *Escherichia coli*. FEMS Microbiol. Lett. **50:**5–9.
45. **Van Soom, C., J. Browaeys, C. Verreth, and J. Vanderleyden.** 1993. Nucleotide sequence analysis of four genes, *hupC*, *hupD*, *hupF* and *hupG*, downstream of the hydrogenase structural genes in *Bradyrhizobium japonicum*. J. Mol. Biol. **234:**508–512.
46. **Vignais, P. M., and B. Toussaint.** 1994. Molecular biology of membrane-bound H_2 uptake hydrogenases. Arch. Microbiol. **172:**2920–2929.
47. **Volbeda, A., M.-H. Charon, C. Piras, E. C. Hatchikian, M. Frey, and J. C. Fontecilla-Camps.** 1995. Crystal structure of the nickel-iron hydrogenase from *Desulfovibrio gigas*. Nature (London) **373:**580–587.
48. **Yanisch-Perron, C., J. Vieira, and J. Messing.** 1985. Improved M13 phage cloning vectors and host strains: nucleotide sequences of the M13mp18 and pUC19 vectors. Gene **33:**103–119.